minerals

Supplementary Materials: An Improved Understanding of Chalcopyrite Leaching Mechanisms: The Influence of Anisotropic Crystal Planes

Zhenlun Wei [1], Xu Yang [1], Wanqing Li [1], Qiang Ma [1], Xiaoyong Wu [1] and Yubiao Li [1,2]

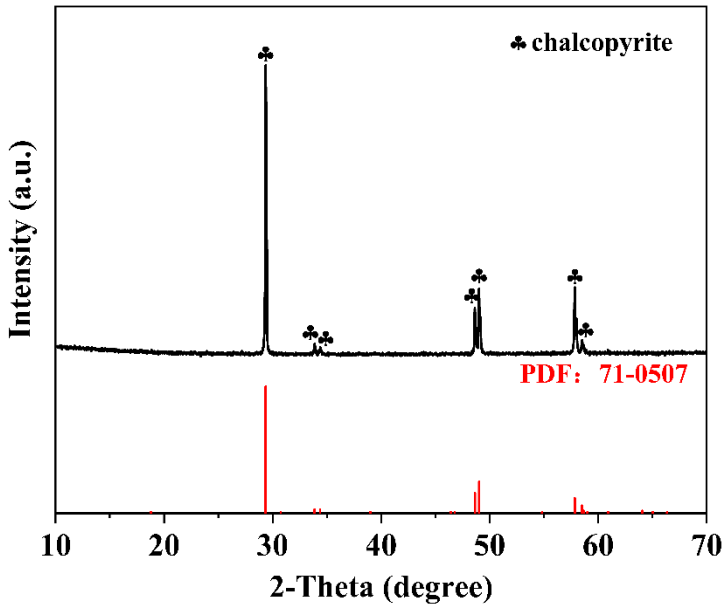

Figure S1. XRD patterns of raw $CuFeS_2$ sample (D8 Advance, Bruker, Germany). The PDF: 71-0507 was the standard XRD pattern of $CuFeS_2$ from Jade 6.0. It was clearly that the diffraction peaks of raw chalcopyrite sample were highly consistent with the standard $CuFeS_2$ XRD pattern (PDF: 71-0507), indicating that the raw $CuFeS_2$ sample in this study was highly purified.

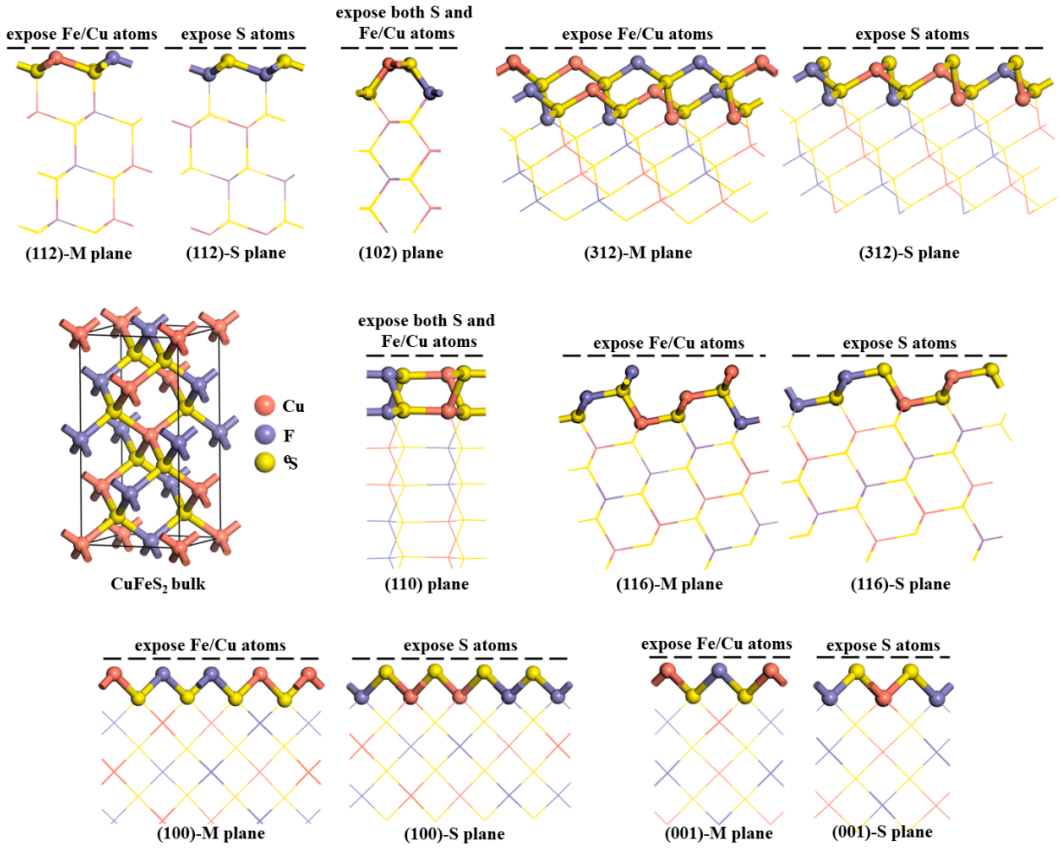

Figure S2. Structure and exposed atoms of $CuFeS_2$ planes.

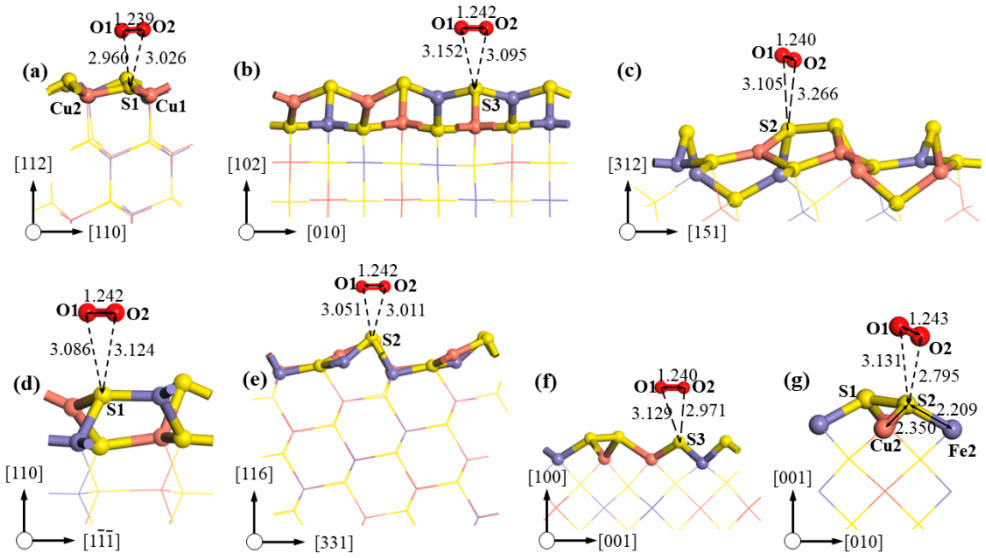

Figure S3. Layout of the adsorption of O_2 at S sites $CuFeS_2$ planes: (**a**) (112)-S plane; (**b**) (102) plane; (**c**) (312)-S plane; (**d**) (110) plane; (**e**) (116)-S plane; (**f**) (100)-S plane; (**g**) (001)-S plane, distances are in Å.

Table S1. Main element contents of $CuFeS_2$ sample determined by XRF (Zetium, PANalytical, Netherland) (wt. %).

Element	Cu	Fe	S	Si	Al	Mg	Ca	Ignition :oss
Content	36.41	31.32	30.21	0.43	0.08	0.16	0.03	1.34

Table S2. Normalized percentage of exposed planes for standard and experimental $CuFeS_2$ particles (%).

Planes	Standard Value	Experimental Value					
		38–75 μm			75–150 μm		
		TM	RM	BM	TM	RM	BM
(112)	54.975	45.696	46.765	47.519	39.618	41.434	48.668
(204)	17.702	16.814	16.977	17.076	16.512	24.436	14.891
(312)	9.841	10.535	9.568	8.828	12.841	7.872	13.583
(220)	9.181	10.048	9.568	10.556	12.691	10.421	10.282
(116)	4.728	6.214	6.189	6.775	7.709	7.035	5.305
(200)	2.419	5.683	5.871	4.828	5.862	4.689	4.064
(001)	1.154	5.010	5.062	4.418	4.767	4.113	3.207

Table S3. Normalized percentage of exposed planes for $CuFeS_2$ particles between standard value and experimental value (%).

Planes	38–75 μm			75–150 μm		
	TM	RM	BM	TM	RM	BM
(112)	−9.279	−8.210	−7.456	−15.357	−13.541	−6.307
(204)	−0.888	−0.725	−0.626	−1.190	6.734	−2.811
(312)	0.694	−0.273	−1.013	3.000	−1.969	3.742
(220)	0.867	0.387	1.375	3.510	1.240	1.101
(116)	1.486	1.461	2.047	2.981	2.307	0.577
(200)	3.264	3.452	2.409	3.443	2.270	1.645
(001)	3.856	3.908	3.264	3.613	2.959	2.053